PNAS RESEARCH ARTICLE | ECOLOGY

Temperature thresholds induce abrupt shifts in biodiversity and ecosystem services in montane ecosystems worldwide

Xiao-Min Zeng[a,b,c], Miguel Berdugo[d], Tadeo Saez-Sandino[e], Dongxue Tao[a,f], Tingting Ren[g], Guiyao Zhou[a], Yu-Rong Liu[b,1], Cesar Terrer[h], Peter B. Reich[e,i,j], and Manuel Delgado-Baquerizo[a,1]

Affiliations are included on p. 8.

Edited by Nils Stenseth, Universitetet i Oslo, Oslo, Norway; received July 12, 2024; accepted March 8, 2025

Montane ecosystems are crucial for maintaining global biodiversity and function that sustain life on our planet. Yet, these ecosystems are highly vulnerable to changing temperatures and may undergo critical transitions under ongoing climate change. What we do not know is to what extent montane biodiversity and ecosystem services will respond to local temperature variations in a gradual versus abrupt manner across global environments. To fill this knowledge gap, we conducted a global synthesis, including 4,462 observations from 290 elevation gradients, to investigate how biodiversity (spanning animals and plants) and ecosystem services (including plant production, soil carbon, and fertility) respond to local temperature variations along elevation gradients. We found that nearly one-third of these gradients exhibited abrupt shifts in multiple biodiversity and ecosystem services in response to local variations in temperature along elevation gradients. More specifically, we showed that once a particular local temperature level (~10 °C for mean annual temperature) was reached, even small increases in temperature resulted in dramatic variations in biodiversity and ecosystem services. We further showed that those abrupt shifts in response to local temperature increases were commonly positive for plant and animal diversity, as well as plant production, while soil carbon and fertility more commonly exhibit negative abrupt trends. Our work, based on the most comprehensive empirical evidence available so far, reveals the pervasive abrupt responses of biodiversity and ecosystem services to local temperature variations in montane ecosystems worldwide, highlighting the highly sensitive nature of montane ecosystems in the context of climate change.

climatic change | local temperature | non-linear responses | thresholds | elevation gradient

Significance

Studying the extent to which local temperature differences induce gradual versus abrupt shifts in montane biodiversity and ecosystem services across global environments is crucial for understanding their responses to global warming. Through a global synthesis of 290 elevation gradients, we found evidence for pervasive abrupt shifts in biodiversity and ecosystem services in response to local temperature variations along elevation gradients. We identified critical temperature thresholds that can trigger abrupt responses of montane biodiversity and ecosystem services to local temperature variations. Our work underscores the urgency of integrating local climatic variability into conservation strategies to safeguard these ecologically vital areas, particularly in regions likely to surpass the identified temperature thresholds in the future.

Montane ecosystems, covering 25% of the Earth's land surface, play a pivotal role in maintaining biodiversity and providing essential ecosystem services (e.g., soil fertility and carbon storage) (1, 2). Unfortunately, these vital ecosystems are increasingly threatened by climate change, posing significant risks to their biodiversity and ecosystem services (3). The distribution of biodiversity and ecosystem services in mountain regions is largely shaped by local temperature variations along elevation gradients (4). Consequently, elevation gradients are often used as natural observatories and model systems to predict the long-term responses of biodiversity and ecosystem services to climate warming (2). Despite a growing body of research on the role of temperature in montane biodiversity and ecosystem services along elevation gradients (5, 6), notable knowledge gaps remain in our understanding of how local temperature variations, particularly temperature thresholds, impact montane biodiversity and ecosystem services. Previous studies in particular regions have shown abrupt shifts in plant species composition at specific temperature thresholds in montane ecosystems (7, 8). For instance, sudden transitions from forest to treeless alpine vegetation (i.e., treelines) often occur where the mean temperature during the growing season is approximately 6 to 7 °C (9). However, it remains unknown whether there are specific temperature thresholds that regulate patterns of montane biodiversity and ecosystem services along elevation gradients at a global scale.

Environmental thresholds, characterized as specific environmental conditions that, once crossed, induce marked shifts in trends, are increasingly regarded as pivotal drivers of biodiversity and ecosystem services (10). For instance, temperature thresholds represent critical points along temperature gradients where the values of ecosystem properties or their relationships with the temperature gradient undergo abrupt shifts (11). Recent research has reported that temperature thresholds linked to particular biodiversity and ecosystem services are more prevalent than previously expected, as evidenced in soil fungal decomposers (12) and ecosystem respiration (13). Understanding the role of temperature thresholds along environmental gradients is crucial for translating the knowledge of

The authors declare no competing interest.

This article is a PNAS Direct Submission.

Copyright © 2025 the Author(s). Published by PNAS. This article is distributed under Creative Commons Attribution-NonCommercial-NoDerivatives License 4.0 (CC BY-NC-ND).

Although PNAS asks authors to adhere to United Nations naming conventions for maps (https://www.un.org/geospatial/mapsgeo), our policy is to publish maps as provided by the authors.

[1]To whom correspondence may be addressed. Email: yrliu@mail.hzau.edu.cn or m.delgado.baquerizo@csic.es.

This article contains supporting information online at https://www.pnas.org/lookup/suppl/doi:10.1073/pnas.2413981122/-/DCSupplemental.

Published April 14, 2025.

Downloaded from https://www.pnas.org by UNIVERSIDAD COMPLUTENSE DE MADRID on May 29, 2025 from IP address 147.96.28.130.

threshold occurrence from spatial variations into temporal changes using space-for-time substitution approaches (14). This can help enhance forecasts of montane biodiversity and ecosystem service responses to future climate warming (12). Furthermore, identifying temperature thresholds and carefully elucidating their underlying mechanisms can help establish effective policy targets to delineate climatic boundaries for montane ecosystems in the current climate crisis (15). However, three main factors have hindered our understanding of the role of temperature thresholds in shaping biodiversity and ecosystem services in montane ecosystems. First, there has been a predominant focus on linear relationships with elevation or temperature (16), neglecting nonlinear relationships. Second, the majority of studies have targeted single aspects of biodiversity and ecosystem services (e.g., a specific organism or function) (17), overlooking their interconnected and systemic nature. Last, most research has been conducted on a limited number of elevation gradients (e.g., single slopes or mountain ranges) (18), restricting the generalizability of findings at a global scale. Closing these knowledge gaps is crucial for gaining a comprehensive understanding of how biodiversity and ecosystem services in montane ecosystems respond to global warming.

Here, we investigated the gradual versus abrupt responses of montane biodiversity and ecosystem services to local temperature variations along elevation gradients, with a particular emphasis on identifying and comprehending temperature thresholds linked to abrupt responses. That is, we aimed to determine whether multiple dimensions of montane biodiversity and ecosystem services exhibit gradual or abrupt responses to local temperature differences, and if these responses are driven by the existence of single or multiple temperature thresholds in montane ecosystems worldwide. To achieve this, we compiled the most comprehensive global database currently available, including 4,462 observations from 290 elevation gradients worldwide (*SI Appendix*, Fig. S1 and Table S1). These elevation gradients encompass a wide range of climate types (e.g., arid, cold, polar, temperate, and tropical), biomes (e.g., forests, grasslands, shrublands), elevation [1 to 5,300 m above sea level (m a.s.l.)], and gradient scale (185 to 4,400 m elevation range) (Fig. 1 and Dataset S1). We gathered information on biodiversity (i.e., the richness and Shannon of plants and animals) and three categories of ecosystem services, including soil carbon (i.e., total and organic soil carbon, and soil organic matter), soil fertility (i.e., the content and availability of soil nutrients such as nitrogen and phosphorus), and plant production (i.e., plant biomass). We focused on these ecosystem properties because i) they deliver some of the fundamental supporting and regulating ecosystem services provided by montane ecosystems (19); ii) they are influenced by a wide array of organisms, including plants and animals (15); and iii) they are relatively easy to measure and are thus frequently reported in the literature.

Montane ecosystems are particularly exposed to gradual or abrupt environmental changes (20), and their responses to such changes may exhibit nonlinearity (21). We hypothesize that abrupt shifts in multiple dimensions of biodiversity and ecosystem services in response to local temperature variations may be common across montane ecosystems worldwide, despite the presence of other well-known response patterns such as linear and curvilinear. Furthermore, we propose that these abrupt responses are linked to temperature thresholds, considering the crucial role of temperature in regulating montane ecosystem properties (4). It is important to note that threshold methods may produce false positives (22); therefore, the careful selection and application of these methods are crucial to avoid misidentifying abrupt shifts. We employed an optimized threshold approach designed to minimize false positives (*SI Appendix*, Fig. S2), enabling a more accurate characterization of abrupt and persistent shifts in the levels (i.e., step shifts) of montane biodiversity and ecosystem services in response to local temperature variations (23). We initially classified and quantified the patterns of biodiversity and ecosystem services in response to local variations in elevation or temperature (i.e., mean annual temperature, MAT), using independent elevation gradients as the units of study. These response patterns were categorized into three main types based on their shapes (linear, curvilinear, and abrupt).

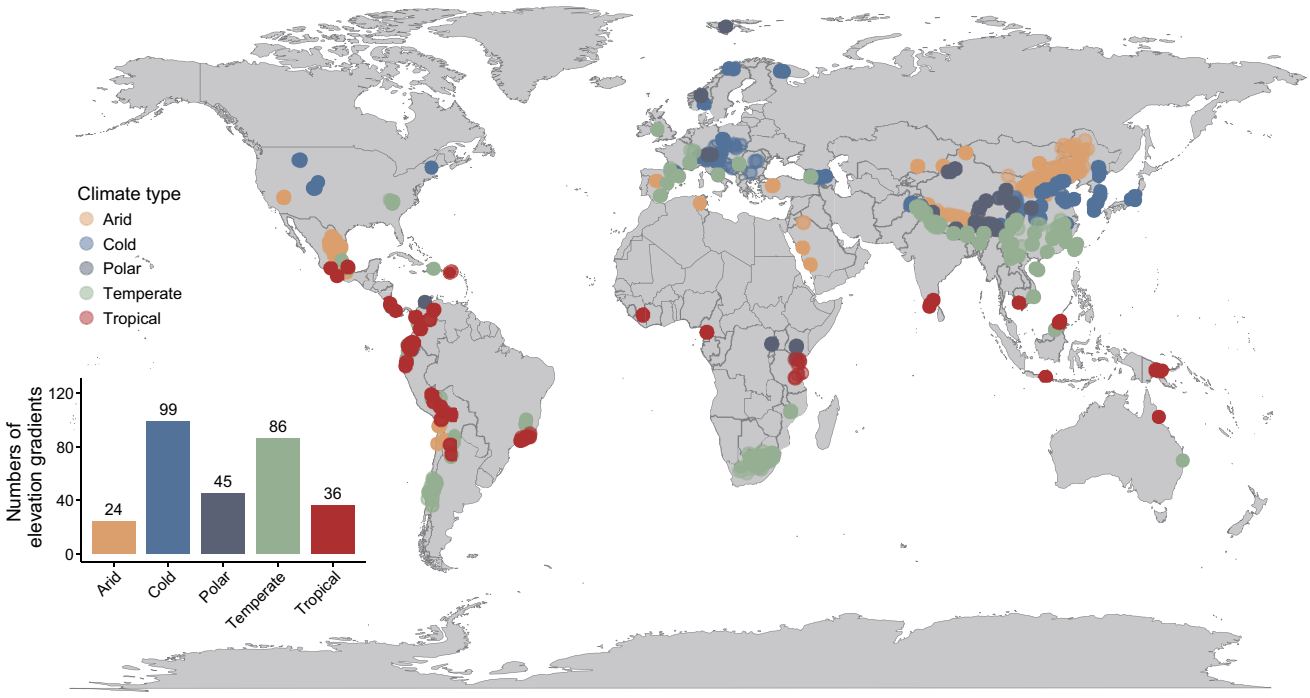

Fig. 1. Global geographical distribution of the sampling sites in this study. The sites are colored based on the Köppen–Geiger climate classification. A total of 4,462 observations were collected from 290 elevation gradients (each with at least seven sampling points) across 270 studies.

Downloaded from https://www.pnas.org by UNIVERSIDAD COMPLUTENSE DE MADRID on May 29, 2025 from IP address 147.96.28.130.

Each type was further divided into three subtypes according to their overall trends (neutral, positive, and negative) (*SI Appendix*, Figs. S2 and S3). Neutral trends indicate that there are no significant variations in these ecosystem properties along elevation or MAT gradients. Subsequently, we tested whether the distribution patterns of biodiversity and ecosystem services along elevation gradients are related to variations in MAT across montane ecosystems worldwide. Finally, we identified the temperature threshold at which abrupt shifts occurred in multiple biodiversity and ecosystem services along MAT gradients.

Results and Discussion

Our study provides evidence that abrupt shifts in montane biodiversity and ecosystem services in response to local variations in temperature and elevation are common (Figs. 2 and 3). Once a particular local temperature level (i.e., ~10 °C for MAT) was reached, even small increases in temperature resulted in marked variations in biodiversity and ecosystem services along elevation gradients. The consistent temperature thresholds observed across elevation gradients worldwide indicate the presence of underlying mechanisms governing these abrupt responses of montane ecosystem properties. These findings are crucial for enhancing our understanding of how montane ecosystem properties may abruptly respond to and provide feedback on global climate change.

Our results first revealed that slightly more than one-third of all elevation gradients (25 to 33%, Fig. 2) exhibited abrupt patterns in multiple biodiversity and ecosystem services, with the exception of the well-known linear and curvilinear patterns (2). In the remaining studied gradients (34 to 58%, Fig. 2), we observed neutral trends, indicating that many montane ecosystems maintained overall stable levels of biodiversity and ecosystem services along the elevation gradients. This may be attributed to the fact that the elevation and MAT ranges of these gradients have not covered the critical thresholds where abrupt shifts may occur (Dataset S1). Consequently, if local temperature surpass these thresholds in the future, the proportion of abrupt shifts in biodiversity and ecosystem services along elevation gradients may increase. These findings expand on previous regional-scale studies that have observed abrupt shifts in a limited number of elevation gradients (24, 25), suggesting the prevalence of abrupt shifts in montane ecosystems worldwide.

We identified local temperature (i.e., MAT) as a crucial predictor of the elevational patterns of montane biodiversity and ecosystem services (*SI Appendix*, Figs. S4 and S5). Our multiple regression analyses and hierarchical partitioning consistently demonstrated that MAT exhibited higher relative importance than other environmental factors (e.g., climate and soil properties) in explaining patterns of biodiversity and ecosystem services across montane ecosystems worldwide. The observed abrupt patterns of montane ecosystem properties are speculated to be linked to local variations in temperature (26, 27). Based on elevation gradient as a reliable proxy for local temperature differences (*SI Appendix*, Fig. S6), we further examined the responses of biodiversity and ecosystem services to local temperature increases along independent elevation gradients. As expected, we also found pervasive abrupt shifts (occurring in 25 to 37% of all elevation gradients, Fig. 3*A*) in biodiversity and ecosystem services along the MAT gradients. Additionally, these abrupt shifts in ecosystem properties along the MAT gradients spatially matched with the abrupt shifts observed along the elevation gradients (Fig. 3*B*). Specifically, 72% of elevation gradients exhibiting abrupt shifts in biodiversity and ecosystem services also showed corresponding abrupt responses to local temperature variations (Fig. 3*B*). Moreover, positive

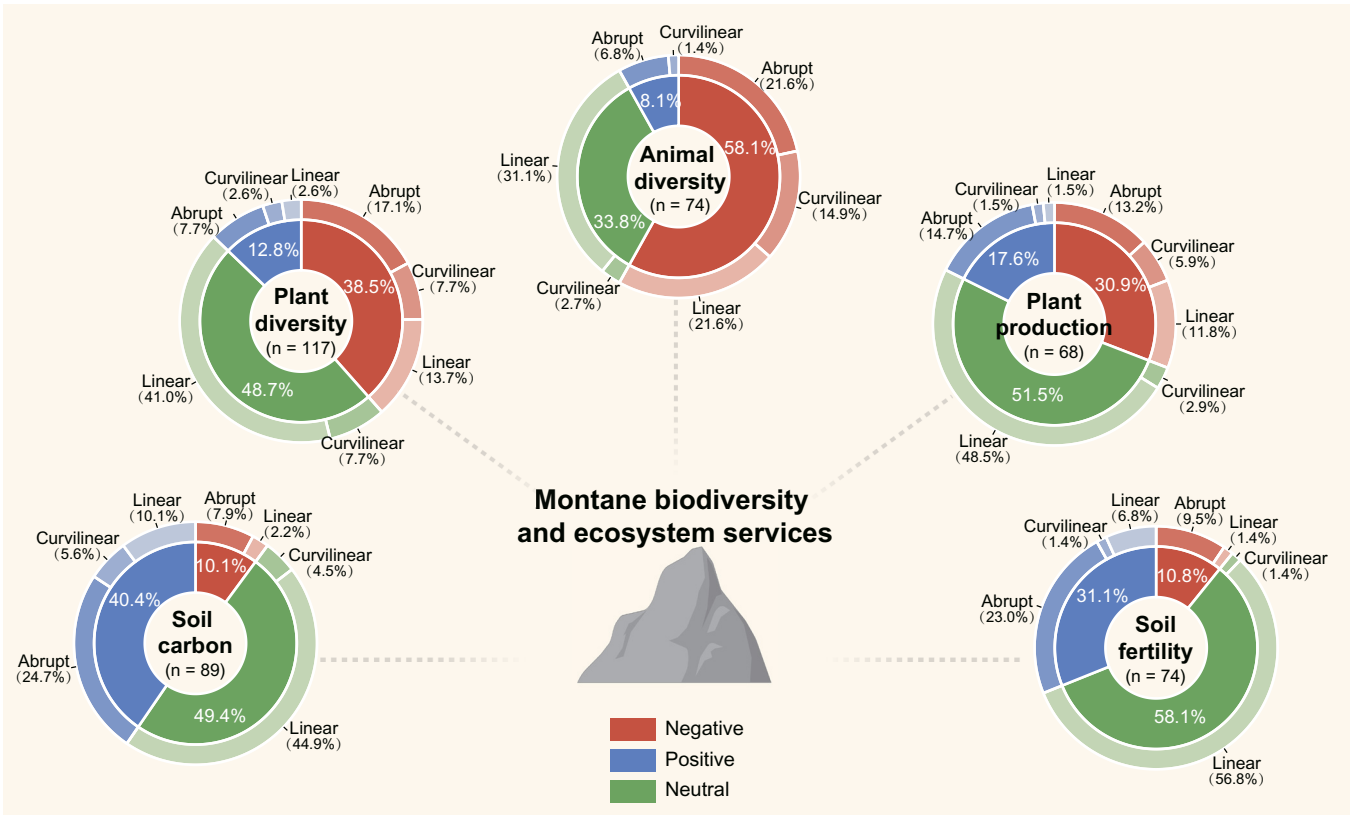

Fig. 2. Abrupt shifts in biodiversity and ecosystem services along elevation gradients in montane ecosystems worldwide. The pie chart illustrates the percentage of neutral (green), positive (blue), and negative (red) trends for biodiversity and ecosystem services in response to variations in elevation. The ring around the pie chart indicates the percentage of linear, curvilinear, and abrupt patterns for each trend. "n" represents the number of elevation gradients.

Downloaded from https://www.pnas.org by UNIVERSIDAD COMPLUTENSE DE MADRID on May 29, 2025 from IP address 147.96.28.130.

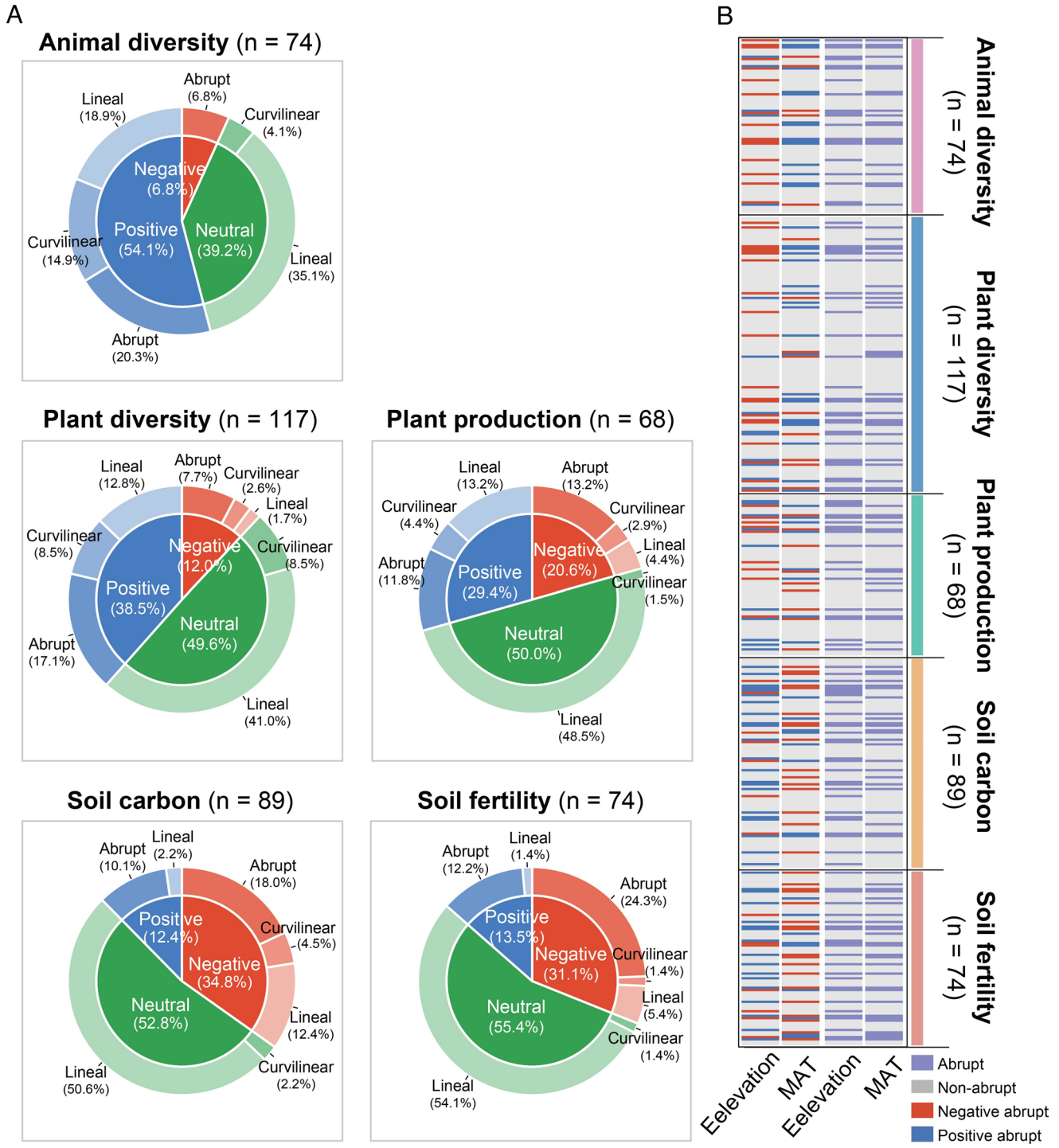

Fig. 3. Abrupt shifts in biodiversity and ecosystem services along temperature gradients in montane ecosystems worldwide. (*A*) Percentage of different response patterns, including linear, curvilinear, and abrupt patterns within neutral (green), positive (blue), and negative (red) trends for biodiversity and ecosystem services in response to local variations in temperature; (*B*) Comparison of response patterns of biodiversity and ecosystem services along corresponding elevation and temperature gradients. This analysis aimed to evaluate whether elevation gradients with abrupt shifts in biodiversity and ecosystem services also exhibited similarly abrupt responses to local temperature variations and whether these abrupt shifts showed opposite trends (negative vs. positive) along corresponding elevation and MAT gradients. MAT. "n" represents the number of elevation gradients.

abrupt shifts along elevation gradients were linked to negative abrupt shifts along MAT gradients, and vice versa (Fig. 3*B*). These results emphasize the critical role of local temperature in shaping abrupt shifts in biodiversity and ecosystem services along elevation gradients, generating a series of discrete thresholds associated with these abrupt responses.

We found pervasive positive abrupt shifts in biodiversity associated with increasing MAT (i.e., decreasing elevation), encompassing both animals (20% of cases) and plants (17% of cases) (Fig. 3*A*). Specifically, we observed abrupt increases in animal and plant diversity in response to local temperature increases once the MAT exceeded the respective thresholds of 13.2 and 10.1 °C (Fig. 4). The observed abrupt increases in biodiversity may be associated with temperature-induced variations in community assembly processes (e.g., environmental filtering, species interactions, and resultant species pools), which are considered

Downloaded from https://www.pnas.org by UNIVERSIDAD COMPLUTENSE DE MADRID on May 29, 2025 from IP address 147.96.28.130.

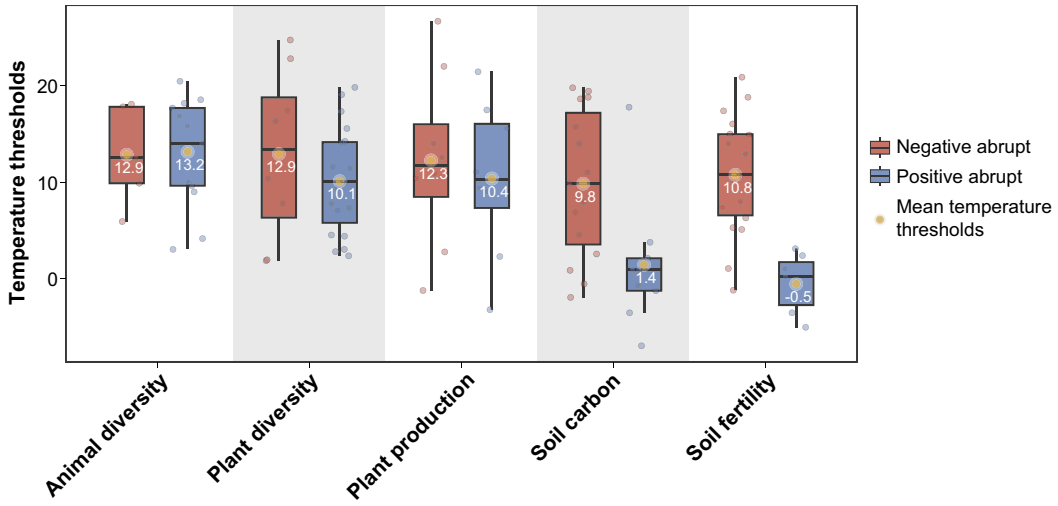

Fig. 4. Temperature thresholds linked to abrupt shifts in biodiversity and ecosystem services along elevation gradients worldwide. Numbers on the boxplot indicate the average values of temperature thresholds identified.

the key mechanisms underlying the abrupt nature of community turnover along environmental gradients (28). This was supported by the view from previous studies that the increased species diversity with decreasing elevation is primarily attributed to increased rates of biological processes and interactions, or increased rates of evolutionary diversification due to local temperature increases (26, 29). Furthermore, the elevation-driven local temperature increases may expand niche spaces and enhance ambient energy and productivity, thereby fostering greater species diversity (30). These factors could ultimately lead to abrupt increases in both plant and animal diversity when the local temperature increases to levels of 10 to 13 °C with decreasing elevation. Additionally, the differences in mean temperature thresholds between animals (~13.2 °C) and plants (~10.1 °C) may reflect disparities in physiological tolerance and energy constraints (31). In general, plants have a broader environmental tolerance compared to animals but are more sensitive to climate change (32, 33). This may explain why plants exhibited abrupt shifts in biodiversity in response to local temperature increases before animals did.

Contrary to the general pattern observed, our analysis also revealed that approximately 7% and 8% of all elevation gradients experienced negative abrupt shifts in animal and plant diversity in response to local temperature increases, respectively (Fig. 3*A*). The abrupt decreases in biodiversity with increasing MAT could be attributed to various factors, including the adverse effects of reduced precipitation offsetting the positive impacts of increased temperatures (34), and particular shifts in vegetation types such as transitions from species-rich grasslands to relatively species-poor forests (35). Moreover, even in natural montane ecosystems, human activities (e.g., overhunting, medicinal plant collection, and logging) tend to intensify at lower elevations, exacerbating the abrupt decreases in animal and plant diversity (5, 36). Notably, the observed negative abrupt shifts in biodiversity suggest that future local warming may lead to potential biodiversity loss in montane ecosystems (37). In parallel, species at risk of disappearing due to warming in mountain regions are often specialists from cold habitats, restricted to mountaintops, making them particularly vulnerable to extinction (38). Hence, there is an urgent need for targeted conservation efforts and adaptive management strategies to mitigate montane biodiversity declines in abrupt hotspots in response to ongoing climate warming.

Apart from biodiversity, we also found pervasive abrupt shifts in ecosystem services in response to local temperature increases across elevation gradients worldwide (Fig. 3). For instance, plant production exhibited similarly frequent positive (12% of cases) and negative (13% of cases) abrupt shifts as MAT increased (Fig. 3*A*). Notably, these abrupt increases coincided with abrupt increases in plant diversity, consistently occurring at a threshold of ~10 °C (Fig. 4). We initially postulated that the abrupt increases in plant production and their co-occurrence with plant diversity might be attributed to triggers related to transitions in vegetation composition along elevation gradients, such as the shift from shrublands or grasslands to forests at treelines (39). However, our results showed that the abrupt increases in plant production associated with crossing treelines have been observed in only a minority of studies (1 out of 8 cases, Dataset S1). In contrast, elevation gradients characterized by entirely forested vegetation exhibited more frequent abrupt increases (7 out of 8 cases, Dataset S1), although the underlying mechanism remains unknown. Further in situ research should be conducted to elucidate why abrupt shifts in plant production occur along elevation gradients within a single vegetation type in response to climate warming. Another possible explanation is that as local temperature increased, abrupt increases in plant diversity enhanced resource utilization complementarity and ecosystem stability (40), ultimately leading to marked increases in plant production. This idea is partially supported by the robust correlation between plant diversity and production (*SI Appendix*, Fig. S7), aligning with previous studies demonstrating the direct effect of plant diversity on plant production (41). Although the relationship between biodiversity and ecosystem functions has been well documented in montane ecosystems (2), its association with abrupt responses in montane ecosystems remains largely unexplored and requires further attention.

Nevertheless, soil carbon (18% of cases) and fertility (24% of cases) consistently exhibited pervasive negative abrupt patterns as MAT increased (Fig. 3). Specifically, nonlinear negative responses of soil carbon to local temperature increases were observed at MAT levels of 9.8 °C (Fig. 4). The observed decline in soil carbon may be a consequence of sudden increases in the abundance of specific microbial groups (e.g., soil fungal decomposers), leading to increased carbon losses through respiration (12, 42). This notion was further supported by the nonlinear relationships between soil respiration and temperature at the global scale (13). Additionally, when local temperature increased to 10.8 °C, a sharp decline in soil fertility was commonly observed across elevation gradients worldwide (Figs. 3 and 4). This may result from the sudden

Downloaded from https://www.pnas.org by UNIVERSIDAD COMPLUTENSE DE MADRID on May 29, 2025 from IP address 147.96.28.130.

increases in the decomposition of soil organic matter with increasing MAT, leading to a drastic decrease in soil fertility (43, 44). Furthermore, the drastic reductions in soil fertility may also be linked to the abrupt declines in soil carbon content (15, 45), supported by the positive relationships observed between soil fertility and soil carbon (*SI Appendix*, Fig. S7). This highlights the strong interconnection between ecosystem properties, indicating that abrupt shifts or changes in specific properties in response to local temperature increases can trigger cascading effects, leading to corresponding variations in other properties across various spatial or temporal scales (11).

Additionally, it is essential to acknowledge that, beyond local temperature, other environmental factors and their interactions may also contribute to abrupt shifts in biodiversity and ecosystem services along the elevation gradients (*SI Appendix*, Figs. S4 and S5). For instance, our results indicated that abrupt declines in plant production were more frequent in mountainous regions of arid areas and less common in tropical mountains (*SI Appendix*, Fig. S8). This suggests that the combination of elevated temperatures and dry conditions is more likely to trigger abrupt reductions in ecosystem services, as supported by previous studies on environmental thresholds across global environmental gradients (12, 15). Future research should consider multiple environmental variables (e.g., temperature and aridity) to elucidate whether and why abrupt shifts in biodiversity and ecosystem services occur in montane ecosystems (23). Furthermore, in situ studies should be conducted to gain mechanistic insights into how local temperature and other environmental factors interact across relevant scales. This integrative approach will enhance our understanding of the complex dynamics governing montane biodiversity and ecosystem services under climate change. Nevertheless, this study provides an important case illustrating the pervasive abrupt responses of biodiversity and ecosystem services to local temperature variations in montane ecosystems worldwide, laying the foundation for future research on threshold response mechanisms in these systems.

Conclusions

Our work provides insights into how local temperature influences montane biodiversity and ecosystem services, highlighting the role of temperature thresholds in triggering abrupt shifts in montane ecosystems worldwide. We identified consistent temperature thresholds (typically ~10 °C for MAT) associated with positive abrupt shifts in animal and plant diversity and plant production, as well as negative abrupt shifts in soil carbon and fertility. Additionally, our results further illustrate how temperature thresholds may regulate abrupt shifts in montane biodiversity and ecosystem services, involving temperature-induced variations in community assembly processes, intricate interactions among ecosystem properties, and soil biogeochemical cycles. In summary, our work reveals the pervasive abrupt responses of biodiversity and ecosystem services to local temperature variations in montane ecosystems worldwide, exposing the vulnerabilities of these ecosystems to global warming.

Materials and Methods

Data Compilation. We collected data from published reports, articles, and reviews on biodiversity and ecosystem services along elevation gradients using the SCOPUS database. We used the following keyword combinations: ("elevation" OR "altitude" OR "mountain" OR "montane") AND ("carbon" OR "nitrogen" OR "phosphorus" OR "biomass" OR "diversity") AND ("soil" OR "terrestrial" OR "land"). Papers had to meet the following criteria to be included in our dataset: i) The data were restricted to studies conducted in natural ecosystems, excluding agricultural or other managed ecosystems; ii) there was at least one selected variable as well as at least seven sampling sites in each elevation gradient; iii) all sampling sites were clearly reported with their specific elevations; iv) soil data were derived from the mineral surface horizons (top ~10 cm); and v) values of selected variables in all sampling sites could be extracted directly from tables, digitized graphs, or contexts. Based on these criteria, we obtained 4,462 observations of biodiversity and ecosystem services from 270 independent publications (*SI Appendix*, Text S1). If measurements were reported multiple times for the same elevation gradient, we only extracted them once to eliminate the influence of pseudoreplicates. Data were extracted directly from the tables, main text, or appendices of the articles, or digitized from figures using GetData Graph Digitizer (http://www.getdata-graph-digitizer.com/download.php). Our global synthesis adhered, to the extent possible, to the PRISMA-EcoEvo guidelines (46). We included a PRISMA flowchart illustrating the processes for selecting the included articles (*SI Appendix*, Fig. S1), as well as a PRISMA-EcoEvo checklist detailing the review and meta-analysis (*SI Appendix*, Table S1).

We first extracted information on biodiversity and ecosystem services, which were partitioned into two categories of biodiversity: plant and animal diversity, and three categories of ecosystem services, including plant production, soil carbon, and soil fertility (*SI Appendix*, Table S2). Among the 270 publications, 70 addressed animal diversity, 107 addressed plant diversity, 67 addressed plant production, 82 addressed soil carbon, and 73 addressed soil fertility (Dataset S1). A list of individual variables that comprise each category can be found in *SI Appendix*, Table S2. Each individual variable was included in only one category of ecosystem properties. In addition, we collected environmental context data with a variety of variables, including geographic information such as latitude, longitude, elevation, and slope, climate factors such as MAT, as well as soil properties such as soil sand content and pH. These variables were selected due to their importance as environmental predictors of montane biodiversity and ecosystem services (5, 47). Missing data were obtained from relevant publications conducted at the same sites or by contacting the corresponding authors. For elevation gradients with a broad geographic distribution of sampling sites, missing data were obtained from global databases using geographical information (i.e., latitude and longitude). Specifically, we extracted MAT and temperature and precipitation seasonality (TSEA and PSEA) from the CHELSA database (http://chelsa-climate.org/). We acknowledge that these macroclimatic data may deviate from actual local conditions. Notably, MAT was critical to our analyses, with only 7.7% of the MAT data sourced from CHELSA (*SI Appendix*, Fig. S9). To evaluate potential impacts, we recalculated the percentages of each classification pattern after excluding gradients for which MAT data were derived from CHELSA. The recalculated results were nearly identical to those obtained from all elevation gradients (*SI Appendix*, Table S3), indicating that the inclusion of these data does not alter the conclusions of our study. The aridity index, which is the ratio of precipitation to potential evapotranspiration, was calculated using interpolations derived from the CHELSA database. Soil properties, including pH and sand content, were obtained from the SoilGrids database (https://www.isric.org/explore/soilgrids). Biomes for each elevation gradient were identified using the MCD12C1 International Geosphere-Biosphere Programme, which mainly include forests, grasslands, and shrublands. In addition, we identified the main climate types for each elevation gradient using the Köppen–Geiger climate classification (48), which encompasses arid, cold, tropical, temperate, and polar regions. This classification was selected for its enhanced accuracy and greater detail, particularly in areas with sharp spatial or elevational gradients (48). It also provides a simplified yet ecologically relevant framework for aggregating complex climate gradients (48, 49), ensuring comparability across studies. Moreover, we incorporated climate information from the published literature for reference (Dataset S1).

Data Analysis.

Assessing montane biodiversity and ecosystem services. Our analyses aimed to provide generalizable insights into how biodiversity and ecosystem services respond to local temperature variations across montane ecosystems worldwide. We did not expect that individual variables within each category of biodiversity and ecosystem services would respond uniformly to local temperature variations, as partially evidenced in previous studies (3, 26). Therefore, we focused on the overall response of each category of biodiversity and ecosystem services rather than on individual variables. To obtain weighted metrics for montane biodiversity

Downloaded from https://www.pnas.org by UNIVERSIDAD COMPLUTENSE DE MADRID on May 29, 2025 from IP address 147.96.28.130.

and ecosystem services across each elevation gradient, we first normalized (log-transformed when needed) and standardized all ecosystem variables using the 0 to 1 transformation along independent elevation gradients. The standardized ecosystem variables within a given category were then averaged to calculate the biodiversity and ecosystem service index (*SI Appendix*, Table S2). For instance, within the category of plant diversity, we averaged the standardized richness and Shannon index.

We evaluated the relative importance of local temperature (i.e., MAT) compared to other environmental factors (i.e., climate and soil properties) in explaining the elevational patterns of biodiversity and ecosystem services across montane ecosystems worldwide. For each elevation gradient, we first employed multiple regression analyses to model the relationships between biodiversity and ecosystem services and various environmental variables (MAT, aridity index, TSEA, PSEA, soil sand content, soil pH, and slope). To address potential multicollinearity and reduce overfitting, we calculated variance inflation factors (VIFs) for each variable using the "car" R package (50). Variables with VIFs > 10 were excluded through a backward selection procedure to mitigate collinearity effects (51). We then calculated the relative importance of each variable in explaining the variance within the multiple regression model using the "relweights" function in R (52). Here, relative importance is defined as the proportionate contribution of each predictor to the model's R^2, considering both unique and combined contributions with other variables (53). Furthermore, hierarchical partitioning was applied to each gradient to quantify the independent contributions of each environmental variable to biodiversity and ecosystem services (54), using the rdacca.hp package (55). Finally, we grouped the results from the multiple regression analysis and hierarchical partitioning to comprehensively assess the relative importance of MAT. Additionally, we conducted Spearman correlations to evaluate the overall relationships among individual biodiversity and ecosystem services, as well as the relationships with MAT and elevation.

Pattern classifications in montane biodiversity and ecosystem services. To classify patterns of biodiversity and ecosystem services along elevation and MAT gradients, we modeled the relationships between these ecosystem properties and elevation, and MAT for each individual elevation gradient. Importantly, we aimed to determine whether these patterns were linear (with monotonic or no-trend shapes), curvilinear (with nonlinear shapes for acceleration or deceleration), or abrupt (with discontinuous shapes that track a particular value of ecosystem properties up to a specific elevation or MAT threshold, after which the values shift suddenly and then maintain until the end of the pattern) (*SI Appendix*, Fig. S3). These distinct patterns are linked to underlying mechanisms that reveal the dynamics of ecosystem functioning, with significant implications for ecosystem stability and monitoring procedures (56, 57). We particularly focused on abrupt patterns characterized by discontinuous shapes (i.e., step shifts), where shifts occur in the level (intercept) rather than in the trend (slope). Such abrupt shifts in biodiversity and ecosystem services indicate that once a sudden shift occurs, the new state remains without immediate reversion (15, 23). The accumulation of such abrupt shifts can be considered as an indication of unstable ecosystems that may transition between alternative states. Identifying such abrupt shifts along elevation gradients provides insights into the prevalence of abrupt responses of biodiversity and ecosystem services to local temperature variations, which are closely linked to montane ecosystem instability under global warming (23). While several recent studies have explored variations in trends (slopes) of individual biodiversity and ecosystem services in mountain ecosystems by breakpoint detection methods (7, 58), research focusing on abrupt shifts in intercepts remains scarce at a global scale.

To perform this classification, we used four statistical models, including no-trend (linked to linear shapes with a single parameter, the intercept, and without a slope), linear (linked to linear shapes with monotonic trends), quadratic (linked to curvilinear shapes and capable of identifying smooth trend or slope shifts), and step models (linked to abrupt shapes), to fit each category of biodiversity and ecosystem services versus elevation or MAT (*SI Appendix*, Figs. S2 and S3). Abrupt shapes can be effectively modeled using segmented (a linear regression with slope shifts at thresholds), step (a linear regression with intercept shifts at thresholds), or stegmented regression (a combination of step and segmented regressions with shifts in both intercept and slope at thresholds) (15). Step regression is especially useful for exploring ecosystem properties that exhibit abrupt shifts or changes that do not immediately revert along spatial or temporal gradients (23). Thus, we applied the step model to fit abrupt shapes, using the "chngpt" package (59) in R, and employed linear and quadratic models to fit linear and curvilinear shapes using the "glm" function of R (60).

To select the best-fitting model for each pattern, we used the corrected Akaike Information Criterion (AICc) due to the limited sample size within each elevation gradient (61). Model selection followed a hierarchical approach (62). First, we considered only statistically significant models ($P < 0.05$). Second, among the multiple significant models, we selected those with the lowest AICc values, as a lower AICc value indicates a better fit. Models with AICc differences of less than 2 (ΔAICc < 2) relative to the minimum AICc were regarded as equally supported in explaining the variation in the response variable. Finally, in cases where multiple models exhibited ΔAICc < 2, we selected the simpler model based on the number of parameters in each model. We considered no-trend models to be the simplest, followed by linear, step, and quadratic models. Prior to fitting, we normalized the ecosystem properties and elevation/MAT values by subtracting the mean and dividing by the SD within each site, allowing coefficient comparisons across models.

To account for potential uncertainty in classifying patterns due to their noisy nature and relatively small sample sizes on each elevation gradient, we employed a bootstrap approach rather than relying on a single regression for each model to identify patterns of biodiversity and ecosystem services along the elevation and MAT gradients. Specifically, we conducted 100 bootstrap iterations to fit models for each gradient and identified the best-fitting model in each iteration. We then recorded the number of times that each model was selected as the best fit out of the 100 bootstraps and used the highest percentage of model selection to determine the best-fit shape for each gradient. This percentage served as a measure of uncertainty in pattern classification (hereafter confidence of pattern classification, Dataset S2). For example, if a model was selected in all 100 bootstraps, the uncertainty would be 0 (on a scale of 0 to 1), indicating high confidence in the pattern classification. This approach allows us to quantify the uncertainty in model selection and evaluate the robustness of the identified patterns across multiple iterations (23). Our results showed high confidence in pattern classification for most gradients (*SI Appendix*, Fig. S10), indicating that the observed patterns of biodiversity and ecosystem services across both elevation and MAT gradients were classified with high accuracy.

Bootstrap and cross-validation are widely used tools for model selection and estimation (63). To evaluate the reliability of these two approaches in this study, we compared their performance using 120 simulated datasets that incorporated known patterns (no-trend, linear, curvilinear, and step) under varying levels of noise and sample sizes. Considering the ability of leave-one-out cross-validation to minimize bias (64), we selected it as the cross-validation method for comparison. Our results indicated that the bootstrap approach described above outperformed cross-validation in classifying patterns, particularly in identifying linear and step patterns (Dataset S3). Specifically, bootstrap correctly identified nearly all linear patterns (97%, 29 out of 30 datasets) and all step patterns (100%, 30 out of 30 datasets). However, cross-validation misclassified 20% (6 out of 30 datasets) of linear patterns as curvilinear and 43.3% (13 out of 30 datasets) of step patterns as linear or curvilinear. These misclassifications were particularly pronounced in datasets with relatively small sample sizes (e.g., n = 7) (Dataset S3). This limitation likely arises because cross-validation requires partitioning the dataset into training and testing subsets for model selection (65). Such partitioning inevitably reduces the amount of data available for training, which can lead to insufficient data for robust model fitting, especially for nonlinear patterns (e.g., step). Conversely, bootstrap resamples from the actual data to generate bootstrapped samples for model selection, enabling more robust model selection even with relatively small datasets (66). Given that many datasets in our study (i.e., elevation gradients) have relatively small sample sizes, bootstrap can provide a more suitable and reliable approach for pattern identification in this context.

To address the misclassification of no-trend patterns as step patterns (Dataset S3), we introduced an additional criterion to improve the accuracy of classifying step patterns (i.e., abrupt shifts). Specifically, we employed the Wald test, a widely used method for evaluating nonlinear models (23, 67), to assess whether the magnitude of change occurring after the change point was substantial enough to meet the definition of a regime shift (i.e., a transition between two states that are significantly different in structure or functioning). If the patterns initially classified as "step" did not meet this criteria (i.e., a Wald test *P*-value > 0.05), they were reassigned to the next best-fit pattern identified through the bootstrap analysis. In other words, after this filtering procedure, the patterns

Downloaded from https://www.pnas.org by UNIVERSIDAD COMPLUTENSE DE MADRID on May 29, 2025 from IP address 147.96.28.130.

were reclassified as linear if they aligned more closely with linear or no-trend models, or as curvilinear if they fit better with quadratic models. This double-check procedure, combining bootstrap analysis with the Wald test, significantly reduced the misclassification rate (Dataset S3), thereby enhancing the robustness and reliability of pattern classification. Additionally, considering the sensitivity of step regressions to influential points or outliers, we explored the incorporation of a Mahalanobis distance-based weighting method into the bootstrap procedure to reduce the impact of outliers (15, 68). However, our results from simulated datasets showed no significant differences between analyses conducted with and without this weighting method, indicating its minimal influence on overall pattern classification (Dataset S3). Consequently, we did not include this weighting method in the final analysis. Our approach allowed us to minimize classification errors and improve the accuracy of identifying abrupt shifts, though noise-induced errors and the potential for error propagation remain possible limitations.

We classified each pattern type (i.e., linear, curvilinear, or abrupt) into three overall trends: neutral (no trend), positive (increasing trend), and negative (decreasing trend) using parameters derived from bootstrapped regressions (Dataset S2). Specifically, we calculated the median values of key model parameters across 100 bootstrap iterations for each gradient. These included the slope parameter (b) for the linear model; the quadratic coefficient (a), the linear coefficient (b), and the 95% CI (bci) for the quadratic model ($y \sim ax^2 + bx + c$); and the *step* parameter for the step model. Linear patterns were classified as positive ($b > 0$) or negative ($b < 0$) based on the sign of the slope parameter, or as neutral when the best-fit model was the no-trend model with only an intercept. Curvilinear patterns were classified as positive ($a > 0$ or $a < 0$ and $b - bci > 0$), negative ($a < 0$ or $a > 0$ and $b + bci < 0$), or shifting ($a > 0$ or $a < 0$ and $b - bci < 0$ and $b + bci > 0$) based on the combination of the quadratic coefficient, the linear coefficient, and its 95% CI. Abrupt patterns were classified as positive ($step > 0$) or negative ($step < 0$) based on the sign of the step parameter (*SI Appendix*, Fig. S2). We then quantified the percentage of elevation and MAT gradients that exhibited linear, curvilinear, or abrupt patterns within neutral, positive, and negative trends.

Furthermore, we identified temperature thresholds only when step models provided a better fit for the data on biodiversity and ecosystem services along independent elevation gradients. To ensure the accuracy of the threshold estimates, we performed 100 bootstrap samplings to identify a set of 100 plausible thresholds for each variable and selected the median value of this set as the final threshold. Additionally, we tested whether the identified threshold significantly affected the intercept of the fitted regressions (i.e., step). Specifically, we conducted bootstrapped linear regressions on either side of the threshold and compared the intercepts before and after it using an unpaired two-sided Mann–Whitney U test (15). In nearly all cases where step regressions provided a better fit, we observed significant differences in the intercepts on both sides of the threshold (Dataset S4). Only data with significant intercept differences across thresholds were included in the final presentation of MAT thresholds.

Data, Materials, and Software Availability. All data and code used in this paper are available in Figshare (69).

ACKNOWLEDGMENTS. M.D.-B. acknowledges the support from TED2021-130908B-C41/AEI/10.13039/501100011033/Unión Europea NextGenerationEU/Plan de Recuperación, Transformación y Resiliencia and from the Spanish Ministry of Science and Innovation for the I + D + i project PID2020-115813RA-I00 funded by MCIN/AEI/10.13039/501100011033. Y.-R.L. acknowledges the support from the National Natural Science Foundation of China (42425701). X.-M.Z. acknowledges the support from the Postdoctoral Fellowship Program (Grade B) of China Postdoctoral Science Foundation (GZB20230822), the China Postdoctoral Science Foundation (2023M743736), and the Hubei Provincial Natural Science Foundation of China (JCZRQN202400547). M.B. acknowledges the support from a Ramón y Cajal Grant from Spanish Ministry of Sciences (RYC2021-031797-I). P.B.R. acknowledges the support from the National Science Foundation Biological Integration Institutes Grant NSF-DBI-2021898. T.S.-S. is supported by the Australian Research Council (DP230101448).

Author affiliations: [a]Laboratorio de Biodiversidad y Funcionamiento Ecosistémico, Instituto de Recursos Naturales y Agrobiología de Sevilla (IRNAS), Consejo Superior de Investigaciones Científicas (CSIC), Sevilla E-41012, Spain; [b]College of Resources and Environment, Huazhong Agricultural University, Wuhan 430070, China; [c]Key Laboratory of Aquatic Botany and Watershed Ecology, Wuhan Botanical Garden, Chinese Academy of Sciences, Wuhan 430074, China; [d]Department of Biodiversity, Ecology and Evolution, Faculty of Biological Sciences, University Complutense of Madrid, Madrid 28040, Spain; [e]Hawkesbury Institute for the Environment, Western Sydney University, Penrith, NSW 2753, Australia; [f]Institute of Grassland Science, Key Laboratory of Vegetation Ecology of the Ministry of Education, Jilin Songnen Grassland Ecosystem National Observation and Research Station, Northeast Normal University, Changchun 130024, China; [g]Department of Ecology, Co-Innovation Center for Sustainable Forestry in Southern China, Nanjing Forestry University, Nanjing 210037, China; [h]Department of Civil and Environmental Engineering, Massachusetts Institute of Technology, Cambridge, MA 02139; [i]Institute for Global Change Biology, and School for Environment and Sustainability, University of Michigan, Ann Arbor, MI 48109; and [j]Department of Forest Resources, University of Minnesota, St. Paul, MN 55108

Author contributions: M.B., Y.-R.L., and M.D.-B. designed research; X.-M.Z., T.S.-S., D.T., and T.R. performed research; X.-M.Z., M.B., G.Z., and M.D.-B. analyzed data; and X.-M.Z., M.B., T.S.-S., G.Z., Y.-R.L., C.T., P.B.R., and M.D.-B. wrote the paper.

1. C. Rahbek *et al.*, Humboldt's enigma: What causes global patterns of mountain biodiversity? *Science* **365**, 1108–1113 (2019).
2. J. Wang *et al.*, Embracing mountain microbiome and ecosystem functions under global change. *New Phytol.* **234**, 1987–2002 (2022).
3. I. Quintero, W. Jetz, Global elevational diversity and diversification of birds. *Nature* **555**, 246–250 (2018).
4. J. R. Mayor *et al.*, Elevation alters ecosystem properties across temperate treelines globally. *Nature* **542**, 91–95 (2017).
5. M. K. Peters *et al.*, Climate-land-use interactions shape tropical mountain biodiversity and ecosystem functions. *Nature* **568**, 88–92 (2019).
6. J. Albrecht *et al.*, Species richness is more important for ecosystem functioning than species turnover along an elevational gradient. *Nat. Ecol. Evol.* **5**, 1582–1593 (2021).
7. K. Albrich, W. Rammer, R. Seidl, Climate change causes critical transitions and irreversible alterations of mountain forests. *Glob. Chang. Biol.* **26**, 4013–4027 (2020).
8. S. Rossi, A. Deslauriers, T. Anfodillo, V. Carraro, Evidence of threshold temperatures for xylogenesis in conifers at high altitudes. *Oecologia* **152**, 1–12 (2007).
9. C. Körner, J. Paulsen, A world-wide study of high altitude treeline temperatures. *J. Biogeogr.* **31**, 713–732 (2004).
10. C. E. Doughty *et al.*, Tropical forests are approaching critical temperature thresholds. *Nature* **621**, 105–111 (2023).
11. M. Berdugo *et al.*, Global ecosystem thresholds driven by aridity. *Science* **367**, 787–790 (2020).
12. Y. Feng *et al.*, Temperature thresholds drive the global distribution of soil fungal decomposers. *Glob. Chang. Biol.* **28**, 2779–2789 (2022).
13. A. S. A. Johnston *et al.*, Temperature thresholds of ecosystem respiration at a global scale. *Nat. Ecol. Evol.* **5**, 487–494 (2021).
14. R. S. L. Lovell, S. Collins, S. H. Martin, A. L. Pigot, A. B. Phillimore, Space-for-time substitutions in climate change ecology and evolution. *Biol. Rev. Camb. Philos. Soc.* **98**, 2243–2270 (2023).
15. J. Zhang *et al.*, Water availability creates global thresholds in multidimensional soil biodiversity and functions. *Nat. Ecol. Evol.* **7**, 1002–1011 (2023).
16. C. J. G. Loewen, D. A. Jackson, B. Gilbert, Biodiversity patterns diverge along geographic temperature gradients. *Glob. Chang. Biol.* **29**, 603–617 (2023).
17. S. N. Kivlin *et al.*, Biogeography of plant-associated fungal symbionts in mountain ecosystems: A meta-analysis. *Divers. Distrib.* **23**, 1067–1077 (2017).
18. W. Chen *et al.*, Soil microbial network complexity predicts ecosystem function along elevation gradients on the Tibetan Plateau. *Soil Biol. Biochem.* **172**, 108766 (2022).
19. F. T. Maestre *et al.*, Plant species richness and ecosystem multifunctionality in global drylands. *Science* **335**, 214–218 (2012).
20. N. Pepin *et al.*, Elevation-dependent warming in mountain regions of the world. *Nat. Clim. Change* **5**, 424–430 (2015).
21. J. Sonne, C. Rahbek, Idiosyncratic patterns of local species richness and turnover define global biodiversity hotspots. *Proc. Natl. Acad. Sci. U.S.A.* **121**, e2313106121 (2024).
22. H. Haines, B. Planque, L. Buttay, M. Hunsicker, Poor performance of regime shift detection methods in marine ecosystems. *ICES J. Mar. Sci.* **82**, fsae103 (2024), 10.1093/icesjms/fsae103.
23. M. Berdugo, J. J. Gaitan, M. Delgado-Baquerizo, T. W. Crowther, V. Dakos, Prevalence and drivers of abrupt vegetation shifts in global drylands. *Proc. Natl. Acad. Sci. U.S.A.* **119**, e2123393119 (2022).
24. Y. Wang, J. Sun, T. M. Lee, Altitude dependence of alpine grassland ecosystem multifunctionality across the Tibetan Plateau. *J. Environ. Manage.* **332**, 117358 (2023).
25. L. Pellissier, B. Fournier, A. Guisan, P. Vittoz, Plant traits co-vary with altitude in grasslands and forests in the European Alps. *Plant Ecol.* **211**, 351–365 (2010).
26. M. K. Peters *et al.*, Predictors of elevational biodiversity gradients change from single taxa to the multi-taxa community level. *Nat. Commun.* **7**, 13736 (2016).
27. J. D. Gay, B. Currey, E. N. J. Brookshire, Global distribution and climate sensitivity of the tropical montane forest nitrogen cycle. *Nat. Commun.* **13**, 7364 (2022).
28. W. K. Cornwell, D. D. Ackerly, Community assembly and shifts in plant trait distributions across an environmental gradient in coastal California. *Ecol. Monogr.* **79**, 109–126 (2009).
29. L. T. Lancaster, A. M. Humphreys, Global variation in the thermal tolerances of plants. *Proc. Natl. Acad. Sci. U.S.A.* **117**, 13580–13587 (2020).
30. D. J. Currie *et al.*, Predictions and tests of climate-based hypotheses of broad-scale variation in taxonomic richness. *Ecol. Lett.* **7**, 1121–1134 (2004).
31. J. Albrecht *et al.*, Plant and animal functional diversity drive mutualistic network assembly across an elevational gradient. *Nat. Commun.* **9**, 3177 (2018).

Downloaded from https://www.pnas.org by UNIVERSIDAD COMPLUTENSE DE MADRID on May 29, 2025 from IP address 147.96.28.130.

32. R. B. Huey *et al.*, Plants versus animals: Do they deal with stress in different ways?. *Integr. Comp. Biol.* **42**, 415–423 (2002).
33. H. Liu, Q. Ye, J. J. Wiens, Climatic-niche evolution follows similar rules in plants and animals. *Nat. Ecol. Evol.* **4**, 753–763 (2020).
34. M. Zhang *et al.*, Constant tree species richness along an elevational gradient of Mt. Bokor, a table-shaped mountain in southwestern Cambodia. *Ecol. Res.* **31**, 495–504 (2016).
35. L. Mumladze, W. Ulrich, Z. Asanidze, G. Japoshvili, An inverse elevational species richness gradient of Caucasian vascular plants and Encyrtidae (Hymenoptera, Chalcidoidea). *Ecoscience* **24**, 75–79 (2017).
36. H. Chen *et al.*, The impacts of climate change and human activities on biogeochemical cycles on the Qinghai-Tibetan Plateau. *Glob. Chang. Biol.* **19**, 2940–2955 (2013).
37. G. R. Kattel, Climate warming in the Himalayas threatens biodiversity, ecosystem functioning and ecosystem services in the 21st century: Is there a better solution? *Biodivers. Conserv.* **31**, 2017–2044 (2022).
38. P. R. Elsen, M. W. Tingley, Global mountain topography and the fate of montane species under climate change. *Nat. Clim. Change* **5**, 772–776 (2015).
39. M. L. Avolio *et al.*, Changes in plant community composition, not diversity, during a decade of nitrogen and phosphorus additions drive above-ground productivity in a tallgrass prairie. *J. Ecol.* **102**, 1649–1660 (2014).
40. P. Garcia-Palacios, N. Gross, J. Gaitan, F. T. Maestre, Climate mediates the biodiversity-ecosystem stability relationship globally. *Proc. Natl. Acad. Sci. U.S.A.* **115**, 8400–8405 (2018).
41. P. Daleo *et al.*, Environmental heterogeneity modulates the effect of plant diversity on the spatial variability of grassland biomass. *Nat. Commun.* **14**, 1809 (2023).
42. A. T. Nottingham, P. Meir, E. Velasquez, B. L. Turner, Soil carbon loss by experimental warming in a tropical forest. *Nature* **584**, 234–237 (2020).
43. Imran, Amanullah, I. Ortas, "The declining trend of soil fertility with climate change and its solution" in *Climate Change and Agriculture: Perspectives, Sustainability and Resilience*, N. Benkeblia, Ed. (Hoboken, NJ, 2022), pp. 179–208.
44. S. Mondal, "Impact of climate change on soil fertility" in *Climate Change and the Microbiome: Sustenance of the Ecosphere*, D. K. Choudhary, A. Mishra, A. Varma, Eds. (Springer International Publishing, Cham, Switzerland, 2021), pp. 551–569.
45. W. R. Wieder, C. C. Cleveland, W. K. Smith, K. Todd-Brown, Future productivity and carbon storage limited by terrestrial nutrient availability. *Nat. Geosci.* **8**, 441–444 (2015).
46. R. E. O'Dea *et al.*, Preferred reporting items for systematic reviews and meta-analyses in ecology and evolutionary biology: A PRISMA extension. *Biol. Rev.* **96**, 1695–1722 (2021).
47. G. Midolo, P. De Frenne, N. Holzel, C. Wellstein, Global patterns of intraspecific leaf trait responses to elevation. *Glob. Chang. Biol.* **25**, 2485–2498 (2019).
48. H. E. Beck *et al.*, Present and future Koppen-Geiger climate classification maps at 1-km resolution. *Sci. Data* **5**, 180214 (2018).
49. H. E. Beck *et al.*, High-resolution (1 km) Koppen-Geiger maps for 1901–2099 based on constrained CMIP6 projections. *Sci. Data* **10**, 724 (2023).
50. J. Fox, S. Weisberg, *An R Companion to Applied Regression* (Sage Publications, 2018).
51. N. Shrestha, Detecting multicollinearity in regression analysis. *Am. J. Appl. Math. Stat.* **8**, 39–42 (2020).
52. R. C. Team, *RA Language and Environment for Statistical Computing* (R Foundation for Statistical Computing, 2020).
53. J. Johnson, A heuristic method for estimating the relative weight of predictor variables in multiple regression. *Multivariate Behav. Res.* **35**, 1–19 (2000).
54. K. Murray, M. M. Conner, Methods to quantify variable importance: Implications for the analysis of noisy ecological data. *Ecology* **90**, 348–355 (2009).
55. J. Lai, Y. Zou, J. Zhang, P. R. Peres-Neto, Generalizing hierarchical and variation partitioning in multiple regression and canonical analyses using the rdacca.hp R package. *Methods Ecol. Evol.* **13**, 782–788 (2022).
56. Z. Ratajczak *et al.*, Abrupt change in ecological systems: Inference and diagnosis. *Trends Ecol. Evol.* **33**, 513–526 (2018).
57. K. N. Suding, R. J. Hobbs, Threshold models in restoration and conservation: A developing framework. *Trends Ecol. Evol.* **24**, 271–279 (2009).
58. A. Hu *et al.*, Mountain biodiversity and ecosystem functions: Interplay between geology and contemporary environments. *ISME J* **14**, 931–944 (2020).
59. Y. Fong, Y. Huang, P. B. Gilbert, S. R. Permar, chngpt: Threshold regression model estimation and inference. *BMC Bioinform.* **18**, 454 (2017).
60. T. Hastie, gam: Generalized Additive Models (R package version 1, The Comprehensive R Archive Network, 2008).
61. M. J. Brewer, A. Butler, S. L. Cooksley, R. Freckleton, The relative performance of AIC, AICCand BIC in the presence of unobserved heterogeneity. *Methods Ecol. Evol.* **7**, 679–692 (2016).
62. D. Anderson, K. Burnham, *Model Selection and Multi-Model Inference* (Springer-Verlag, New York, NY, 2004).
63. R. Kohavi, A study of cross-validation and bootstrap for accuracy estimation and model selection. *IJCAI* **14**, 1137–1145 (1995).
64. L. A. Yates, Z. Aandahl, S. A. Richards, B. W. Brook, Cross validation for model selection: A review with examples from ecology. *Ecol. Monogr.* **93**, e1557 (2023).
65. S. Bates, T. Hastie, R. Tibshirani, Cross-validation: What does it estimate and how well does it do it? *J. Am. Stat. Assoc.* **119**, 1434–1445 (2024).
66. E. Amalnerkar, T. H. Lee, W. Lim, Reliability analysis using bootstrap information criterion for small sample size response functions. *Struct. Multidiscip. Optim.* **62**, 2901–2913 (2020).
67. Y. Fong, C. Di, Y. Huang, P. B. Gilbert, Model-robust inference for continuous threshold regression models. *Biometrics* **73**, 452–462 (2017).
68. X. Liu, F. Gao, Y. Wu, Z. Zhao, Detecting outliers and influential points: an indirect classical Mahalanobis distance-based method. *J. Stat. Comput. Simul.* **88**, 2013–2033 (2018).
69. X. Zeng *et al.*, Temperature thresholds induce abrupt variations in biodiversity and ecosystem services in montane ecosystems worldwide. https://figshare.com/s/0f404c8cb205eb705042. Deposited 7 February 2025.

Downloaded from https://www.pnas.org by UNIVERSIDAD COMPLUTENSE DE MADRID on May 29, 2025 from IP address 147.96.28.130.